

一种新的硅基晶体 BaH_2SiO_4 的结构和性能

陈乾旺^{*.1,3} 周忠远² Mak C. L.¹ Wong K. H.¹ 唐恕一³ 朱挺³

(¹ 香港理工大学应用物理系, 香港)

(² 香港理工大学生物与化学应用技术系, 香港)

(³ 中国科学技术大学材料科学与工程系, 合肥 230026)

本文报道了采用水热法生长 BaH_2SiO_4 单晶的实验结果。它属三斜晶系, 空间群为 $P\bar{1}$, 晶胞参数为: $a = 7.079$, $b = 7.362$, $c = 7.5824\text{\AA}$, $\alpha = 89.64^\circ$, $\beta = 88.785^\circ$, $\gamma = 88.23^\circ$ 。原子力显微镜(AFM)和P-E铁电回线测量显示该材料具有铁电性, 沿(010)方向极化强度和矫顽力分别为 $0.882 \mu\text{C} \cdot \text{cm}^{-2}$ 和 $1.12 \text{kV} \cdot \text{cm}^{-1}$ 。研究显示铁电性来源于材料中的氢键。

关键词: 铁电晶体 硅基材料 水热技术 晶体结构

分类号: 0613.72

Properties and Crystal Structure of a Novel Silicate Single Crystal: BaH_2SiO_4

CHEN Qian-Wang^{*.1,3} ZHOU Zhong-Yuan² Mak C. L.¹ Wong K. H.¹ TANG Shu-Yi³ ZHU Ting³

(¹ Department of Applied Physics, The Hong Kong Polytechnic University, Hong Kong)

(² Department of ABCT, The Hong Kong Polytechnic University, Hong Kong)

(³ Department of Materials Science and Engineering, University of Science and Technology of China, Hefei 230026)

We have grown single crystals of BaH_2SiO_4 by hydrothermal method. The crystal structure has been studied by direct method. Based on the 1792 unique reflections collected using $\text{MoK}\alpha$ of X-ray radiation and a CCD-based detector, it is refined to an agreement index (R_1) of 6.36% . The cell is triclinic with dimensions: $a = 7.079$, $b = 7.362$, $c = 7.5824\text{\AA}$ and $\alpha = 89.640^\circ$, $\beta = 88.785^\circ$, $\gamma = 88.230^\circ$. There are four unit cells of BaH_2SiO_4 in the cell, with space group $P\bar{1}$.

Keywords: ferroelectric crystal silicate materials hydrothermal technology crystal structure

0 Introduction

The ferroelectric random-access memories (FRAM) are expected to replace magnetic core memory, magnetic bubble memory, and electrically erasable read-only memory for many applications^[1] . There is a need to develop ferroelectric RAM devices that can be integrated with standard microelectronics. Conventional semiconductor technology is largely based on crystalline silicon, which has a diamond structure

with no net dipole polarization necessary for a ferroelectric effect. This has stimulated vigorous studies to develop perovskite-based ferroelectric memory devices for Si metal-oxide-semiconductor field-effect transistor (MOSFET) structures. A Si-based ferroelectric materials surely will be preferred in the integration with MOSFET structures, as compared with non-Si based systems. For example, $\text{Pb}(\text{Zr}, \text{Ti})\text{O}_3$ (PZT) is a promising candidate for ferroelectric random-access

收稿日期: 2001-10-08。收修改稿日期: 2001-11-13。

* 通讯联系人。E-mail: cqw@ustc.edu.cn

第一作者: 陈乾旺, 男, 36岁, 教授; 研究方向: 功能材料。

memory^[1]. However, the interface reactions between this ferroelectric material and the Si substrates (generation of mobile ions and low retention) make it difficult to obtain a good ferroelectric/Si interface in the metal/ferroelectric/semiconductor field-effect transistors gate^[2-4]. A device fabricated with Si-based ferroelectric material can eliminate the possible contamination of an Si IC wafer line by the metal ions in the non-Si-based ferroelectric(e. g. PZT). This will greatly simplify the technique in a ferroelectric RAM production. The ability to extend the use of silicon-based material as a ferroelectric thin film will therefore enable the realization of ferroelectric memory that are compatible with almost all of the microelectronic industry. Unfortunately, no Si-based ferroelectric material has ever been reported so far. Here we report the growth and structure determination of BaH₂SiO₄ single crystal, which shows highly lossy linear dielectric response at room temperature along (100) direction. It is expected to observe ferroelectricity in (010) and (001) direction of the crystal.

1 Experimental

1.1 Preparation of Single Crystal

Hydrothermal processes, primarily developed to study the material formation mechanism, have been widely used for new materials syntheses^[5-7]. Due to the relatively high pressure, variable pH value and precise chemical composition control in the system, some materials can be formed at lower temperatures than that is needed in solid state reactions. In this experiment, single crystals of BaH₂SiO₄ were grown on a glass substrate by a hydrothermal method. A commercially available glass (SiO₂: 77.2%) plate (3cm × 2cm) was coated with a mixture of barium and silicon oxide sol (Ba : Si = 1 : 1), and was put in a Teflon vessel, which was filled with 1.0mol · L⁻¹ Ba(OH)₂ solution. The Teflon vessel was put into an air-tight stainless steel tank and held at a temperature of 160°C for 6 hrs. It was then cooled to room temperature naturally. Small white crystals with size 3 × 1 × 0.5mm were found lying on the glass plate. Elec-

tron energy dispersive spectroscopy (EDX) analysis of the crystals showed barium and silicon as major constituents with no other detectable metal elements. The composition was determined to be Ba: Si = 1: 1 in mole ratio.

1.2 Unit Cell and Symmetry

A Bruker AXS system (SMART 1000, MoKα X-ray radiation and a CCD-based detector) was used to determine the unit cell and symmetry of BaH₂SiO₄. The cell was found to be triclinic with dimensions of the unit cell being $a = 7.0790$, $b = 7.3620$, $c = 7.5824\text{Å}$ and $\alpha = 89.640^\circ$, $\beta = 88.785^\circ$, $\gamma = 88.230^\circ$. The density calculated on the basis of four units of BaH₂SiO₄ per cell was $3.876\text{g} \cdot \text{cm}^{-3}$.

1.3 X-ray Intensities

The intensities of a total of 2640 reflections with $2\theta \leq 55.08^\circ$ were measured from the crystal. 1792 independent reflections were obtained. Lorentz and polarization corrections were applied. An absorption correction was applied with the program SADABS (semi-empirical). The structure was solved from three-dimensional Patterson and difference Fourier syntheses. It was refined by full-matrix least-squares calculations. The final agreement indices were $R = \sum ||F_0| - |F_c|| / \sum |F_0| = 0.0636$ and $R_{\text{w}} = [\sum w(|F_0| - |F_c|)^2 / \sum wF_0^2]^{1/2} = 0.1605$. The coordinates and anisotropic displacement parameters are given in Table 1 and Table 2, respectively.

2 Discussion

2.1 Description of the Structure

As shown in Fig. 1, each unit cell contains four-isolated SiO₄ tetrahedron linked by barium atoms. Fig. 2 shows the atomic coordinates and atom numbering in the cell. The bond lengths and angles are given in Table 3. The Si-O tetrahedron is almost regular, the Si-O distances range only from 1.598 to 1.665Å and the O-Si-O angles from 105.2 to 113.7°. The average Si-O bond length of 1.632Å is abnormally short when compared with 1.860Å, the sum of the Goldschmidt radii corrected for the reduction of the coordination number from six to four (Pauling, 1940). The Si-O

Table 1 Atomic Coordinates ($\times 10^4$) and Equivalent Isotropic Displacement Parameters ($\text{\AA}^2 \times 10^3$) for BaH_2SiO_4 Crystal

	<i>x</i>	<i>y</i>	<i>z</i>	<i>U</i> (eq)		<i>x</i>	<i>y</i>	<i>z</i>	<i>U</i> (eq)
Ba(1)	4348(1)	1886(1)	7995(1)	12(1)	Ba(2)	1285(1)	2602(1)	12912(1)	12(1)
Si(1)	9262(2)	2415(2)	7922(2)	12(1)	Si(2)	6092(2)	2704(2)	12895(2)	10(1)
O(1)	10644(6)	3389(6)	6477(5)	18(1)	O(2)	7846(6)	4076(6)	8707(5)	17(1)
O(3)	7994(6)	955(5)	6986(5)	14(1)	O(4)	10548(6)	1567(6)	9489(5)	15(1)
O(5)	7547(6)	1089(6)	13640(5)	17(1)	O(6)	4741(6)	3398(6)	14533(5)	15(1)
O(7)	4847(6)	1805(6)	11407(5)	14(1)	O(8)	7380(6)	4352(6)	12116(6)	18(1)

U(eq) is defined as one third of the trace of the orthogonalized *U*_{ij} tensor.

Table 2 Anisotropic Displacement Parameters ($\text{\AA}^2 \times 10^3$) for the Crystal of BaH_2SiO_4 .

	<i>U</i> ₁₁	<i>U</i> ₂₂	<i>U</i> ₃₃	<i>U</i> ₁₂	<i>U</i> ₁₃	<i>U</i> ₂₃		<i>U</i> ₁₁	<i>U</i> ₂₂	<i>U</i> ₃₃	<i>U</i> ₁₂	<i>U</i> ₁₃	<i>U</i> ₂₃
Ba(1)	12(1)	13(1)	13(1)	0(1)	-2(1)	0(1)	Ba(2)	12(1)	13(1)	13(1)	-1(1)	-2(1)	0(1)
Si(1)	10(1)	14(1)	11(1)	-2(1)	-3(1)	0(1)	Si(2)	10(1)	11(1)	10(1)	-3(1)	-3(1)	-1(1)
O(1)	19(2)	21(2)	13(2)	2(2)	11(2)	-5(2)	O(2)	23(2)	18(2)	10(2)	1(2)	0(2)	7(2)
O(3)	18(2)	12(2)	13(2)	-11(2)	-3(2)	-1(2)	O(4)	17(2)	18(2)	11(2)	0(2)	-3(2)	-3(2)
O(5)	23(2)	17(2)	11(2)	11(2)	-3(2)	5(2)	O(6)	12(2)	19(2)	14(2)	-7(2)	1(2)	-2(2)
O(7)	15(2)	17(2)	11(2)	-7(2)	-5(2)	-4(2)	O(8)	19(2)	20(2)	14(2)	1(2)	2(2)	-7(2)

The anisotropic displacement factor exponent takes the form: $-2\pi[4ha^*]^2 U_{11} + \dots + 2hka^* b^* U_{12}]$

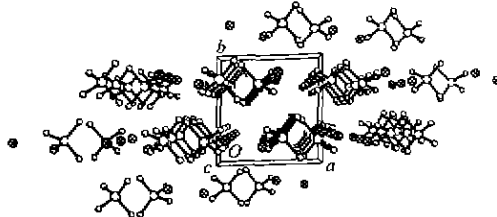


Fig. 1 Structure of showing the connection of Si-O tetrahedron and the environment of Ba₁, Ba₂

bonds in BaH_2SiO_4 must therefore have a considerable covalent character. The oxygen-oxygen distance (2.6602 Å) within the tetrahedron lies reasonably close to the normal value of 2.8 Å. The Ba-O distances may be arbitrarily divided into two classes: oxygen atoms at distances less than 2.909 Å are classed nearest neighbours in contact with barium, and oxygen atoms at distances between 2.909 Å and 3.245 Å are classed as second-nearest neighbours. In BaH_2SiO_4 , Ba₁ is coordinated by nine oxygen atoms, four of which are nearest neighbours. The second barium, Ba₂, is also coordinated by nine oxygen atoms and is in contact with six of them Fig. 2.

2.2 Polarization Properties

The P-E hysteresis loop along (100) direction of the crystal is not monotonic (not shown), which shows highly lossy linear dielectric response. It could be, therefore, not indicative of a ferroelectric hysteresis.

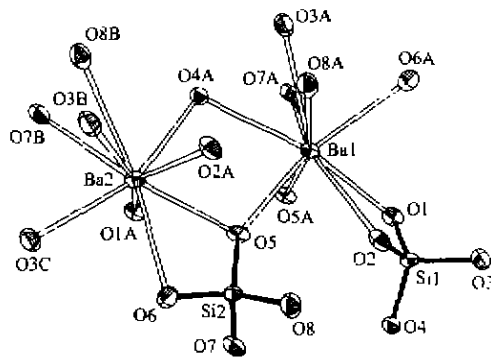


Fig. 2 Atomic coordinates and atom numbering in the unit cell. However, Atomic Force Microscopy (AFM) results show there exists spontaneous polarization in this material. The surface morphology of the BaH_2SiO_4 single crystal was measured by AFM and was shown in Fig. 3a. AFM was also used to image the state of the remanent polarization of the single crystal. Fig. 3b shows the two-dimensional domain image from the same area shown in Fig. 3a. We observed clearly distinguishable positive and negative voltage signals along the line A-B (not shown). Effort is being made to measure the P-E hysteresis loop along (010) and (001) directions of the crystal, in which ferroelectric hysteresis loop correspondent to the ferroelectric domain observed in AFM studies could be obtained.

It is evident that for the ratio of the number of oxygen atoms to barium atoms is not sufficient to allow

Table 3 Bond Lengths (Å) and Angles (°) for the Crystal of BaH₂SiO₄

Ba(1)-O(7)	2.619(4)	Ba(1)-O(3)	2.744(4)	Ba(1)-O(7) #1	2.795(4)
Ba(1)-O(6) #2	2.856(4)	Ba(1)-O(5) #1	2.902(4)	Ba(1)-O(4) #3	2.912(4)
Ba(1)-O(8) #4	2.994(4)	Ba(1)-O(2)	3.055(4)	Ba(1)-O(1) #3	3.059(4)
Ba(1)-Si(2) #1	3.4746(17)	Ba(1)-Si(1)	3.5115(17)	Ba(1)-Si(1) #3	3.6110(17)
Ba(2)-O(3) #1	2.654(4)	Ba(2)-O(4) #3	2.774(4)	Ba(2)-O(1) #5	2.792(4)
Ba(2)-O(7)	2.793(4)	Ba(2)-O(2) #4	2.809(4)	Ba(2)-O(6)	2.840(4)
Ba(2)-O(5) #3	2.943(5)	Ba(2)-O(8) #3	3.083(4)	Ba(2)-O(1) #4	3.245(4)
Ba(2)-Si(2)	3.4059(17)	Ba(2)-Si(2) #3	3.6747(17)	Ba(2)-Si(1) #4	3.7279(19)
Si(1)-O(3)	1.600(4)	Si(1)-O(4)	1.622(4)	Si(1)-O(1)	1.631(4)
Si(1)-O(2)	1.662(4)	Si(1)-Ba(1) #6	3.6110(17)	Si(1)-Ba(2) #4	3.7279(19)
Si(1)-Ba(2) #1	3.7844(19)	Si(2)-O(7)	1.604(4)	Si(2)-O(6)	1.627(4)
Si(2)-O(8)	1.639(4)	Si(2)-O(5)	1.653(4)	Si(2)-Ba(1) #1	3.4746(17)
Si(2)-Ba(2) #6	3.6747(17)	O(1)-Ba(2) #7	2.792(4)	O(1)-Ba(1) #6	3.059(4)
O(1)-Ba(2) #4	3.245(4)	O(2)-Ba(2) #4	2.809(4)	O(3)-Ba(2) #1	2.654(4)
O(4)-Ba(2) #6	2.774(4)	O(4)-Ba(1) #6	2.912(4)	O(5)-Ba(1) #1	2.902(4)
O(5)-Ba(2) #6	2.943(4)	O(6)-Ba(1) #8	2.856(4)	O(7)-Ba(1) #1	2.795(4)
O(8)-Ba(1) #4	2.994(4)	O(8)-Ba(2) #6	3.083(4)		
O(7)-Ba(1)-O(3)	97.31(12)	O(7)-Ba(1)-O(7) #1	78.20(13)	O(3)-Ba(1)-O(7) #1	68.71(12)
O(7)-Ba(1)-O(6) #2	154.20(12)	O(3)-Ba(1)-O(6) #2	75.95(11)	O(7) #1-Ba(1)-O(6) #2	120.41(12)
O(7)-Ba(1)-O(5) #1	119.04(12)	O(3)-Ba(1)-O(5) #1	98.58(12)	O(7) #1-Ba(1)-O(5) #1	54.70(11)
O(6) #2-Ba(1)-O(5) #1	86.73(12)	O(7)-Ba(1)-O(4) #3	75.93(12)	O(3)-Ba(1)-O(4) #3	159.97(12)
O(7) #1-Ba(1)-O(4) #3	91.34(12)	O(6) #2-Ba(1)-O(4) #3	118.03(11)	O(5) #1-Ba(1)-O(4) #3	69.67(12)
O(7)-Ba(1)-O(8) #4	95.90(12)	O(3)-Ba(1)-O(8) #4	125.25(12)	O(7) #1-Ba(1)-O(8) #4	165.76(12)
O(6) #2-Ba(1)-O(8) #4	69.70(11)	O(5) #1-Ba(1)-O(8) #4	119.96(12)	O(4) #3-Ba(1)-O(8) #4	74.59(12)
O(7)-Ba(1)-O(2)	72.90(12)	O(3)-Ba(1)-O(2)	53.99(12)	O(7) #1-Ba(1)-O(2)	109.69(11)
O(6) #2-Ba(1)-O(2)	83.37(11)	O(5) #1-Ba(1)-O(2)	152.38(12)	O(4) #3-Ba(1)-O(2)	137.32(11)
O(8) #4-Ba(1)-O(2)	80.37(11)	O(7)-Ba(1)-O(1) #3	120.68(12)	O(3)-Ba(1)-O(1) #3	140.99(11)
O(7) #1-Ba(1)-O(1) #3	124.14(11)	O(6) #2-Ba(1)-O(1) #3	65.97(11)	O(5) #1-Ba(1)-O(1) #3	71.88(11)
O(4) #3-Ba(1)-O(1) #3	52.46(11)	O(8) #4-Ba(1)-O(1) #3	48.11(12)	O(2)-Ba(1)-O(1) #3	125.86(11)
O(7)-Ba(1)-Si(2) #1	101.19(9)	O(3)-Ba(1)-Si(2) #1	79.41(9)	O(7) #1-Ba(1)-Si(2) #1	26.97(8)
O(6) #2-Ba(1)-Si(2) #1	101.94(9)	O(5) #1-Ba(1)-Si(2) #1	28.27(9)	O(4) #3-Ba(1)-Si(2) #1	83.42(9)
O(8) #4-Ba(1)-Si(2) #1	147.88(9)	O(2)-Ba(1)-Si(2) #1	130.63(8)	O(1) #3-Ba(1)-Si(2) #1	99.84(8)
O(7)-Ba(1)-Si(1)	82.15(9)	O(3)-Ba(1)-Si(1)	26.15(9)	O(7) #1-Ba(1)-Si(1)	86.21(9)
O(6) #2-Ba(1)-Si(1)	81.59(8)	O(5) #1-Ba(1)-Si(1)	124.65(9)	O(4) #3-Ba(1)-Si(1)	157.97(8)
O(8) #4-Ba(1)-Si(1)	105.98(9)	O(2)-Ba(1)-Si(1)	28.24(8)	O(1) #3-Ba(1)-Si(1)	143.41(8)
Si(2) #1-Ba(1)-Si(1)	103.17(4)	O(1) #3-Ba(1)-Si(1) #3	99.85(9)	O(3)-Ba(1)-Si(1) #3	160.77(9)
O(7) #1-Ba(1)-Si(1) #3	106.45(9)	O(6) #2-Ba(1)-Si(1) #3	91.94(8)	O(5) #1-Ba(1)-Si(1) #3	65.37(9)
O(4) #3-Ba(1)-Si(1) #3	26.09(8)	O(8) #4-Ba(1)-Si(1) #3	61.43(9)	O(2)-Ba(1)-Si(1) #3	140.48(8)
O(1) #3-Ba(1)-Si(1) #3	26.70(8)	Si(2) #1-Ba(1)-Si(1) #3	88.78(4)	Si(1)-Ba(1)-Si(1) #3	167.34(5)
O(3) #1-Ba(2)-O(4) #3	77.66(12)	O(3) #1-Ba(2)-O(1) #5	101.76(12)	O(4) #3-Ba(2)-O(1) #5	159.29(12)
O(3) #1-Ba(2)-O(7)	70.01(12)	O(4) #3-Ba(2)-O(7)	75.55(12)	O(1) #5-Ba(2)-O(7)	124.10(12)
O(3) #1-Ba(2)-O(2) #4	146.11(12)	O(4) #3-Ba(2)-O(2) #4	83.41(12)	O(1) #5-Ba(2)-O(2) #4	105.68(12)
O(7)-Ba(2)-O(2) #4	78.22(12)	O(3) #1-Ba(2)-O(6)	92.91(12)	O(4) #3-Ba(2)-O(6)	130.75(12)
O(1) #5-Ba(2)-O(6)	69.86(12)	O(7)-Ba(2)-O(16)	56.12(11)	O(2) #4-Ba(2)-O(6)	78.49(12)
O(3) #1-Ba(2)-O(5) #3	76.69(12)	O(4) #3-Ba(2)-O(15) #3	82.74(12)	O(1) #5-Ba(2)-O(15) #3	77.06(12)
O(7)-Ba(2)-O(5) #3	143.28(12)	O(2) #4-Ba(2)-O(15) #3	128.60(12)	O(6)-Ba(2)-O(5) #3	142.47(12)
O(3) #1-Ba(2)-O(8) #3	124.10(12)	O(4) #3-Ba(2)-O(8) #3	75.01(12)	O(1) #5-Ba(2)-O(18) #3	88.89(12)
O(7)-Ba(2)-O(8) #3	142.81(11)	O(2) #4-Ba(2)-O(8) #3	76.30(12)	O(6)-Ba(2)-O(8) #3	140.94(12)
O(5) #3-Ba(2)-O(8) #3	52.31(11)	O(3) #1-Ba(2)-O(11) #4	163.04(11)	O(4) #3-Ba(2)-O(1) #4	107.69(11)
O(1) #5-Ba(2)-O(1) #4	67.39(13)	O(7)-Ba(2)-O(1) #4	126.69(11)	O(2) #4-Ba(2)-O(11) #4	50.59(11)
O(6)-Ba(2)-O(1) #4	95.18(11)	O(5) #3-Ba(2)-O(1) #4	87.88(11)	O(8) #3-Ba(2)-O(1) #4	45.82(11)
O(3) #1-Ba(2)-Si(2)	81.91(9)	O(4) #3-Ba(2)-Si(2)	102.63(9)	O(1) #5-Ba(2)-Si(2)	97.73(9)

O(7)-Ba(2)-Si(2)	27.8118	O(2)#4-Ba(2)-Si(2)	75.09(9)	O(6)-Ba(2)-Si(2)	28.3918
O(5)#3-Ba(2)-Si(2)	156.3119	O(8)#3-Ba(2)-Si(2)	151.37(9)	O(1)#4-Ba(2)-Si(2)	111.7318
O(3)#1-Ba(2)-Si(2) #3	100.5219	O(4)#3-Ba(2)-Si(2) #3	77.65(9)	O(1)#5-Ba(2)-Si(2) #3	82.1819
O(7)-Ba(2)-Si(2) #3	152.9118	O(2)#4-Ba(2)-Si(2) #3	102.56(9)	O(6)-Ba(2)-Si(2) #3	150.9518
O(5)#3-Ba(2)-Si(2) #3	26.0518	O(8)#3-Ba(2)-Si(2) #3	26.2618	O(1)#4-Ba(2)-Si(2) #	365.9518
Si(2)-Ba(2)-Si(2) #3	177.5515	O(3)#1-Ba(2)-Si(2) #4	170.55(9)	O(4)#3-Ba(2)-Si(2) #4	95.7219
O(1)#5-Ba(2)-Si(1) #4	86.83(9)	O(7)-Ba(2)-Si(2) #4	101.99(9)	O(2)#4-Ba(2)-Si(2) #4	24.70(9)
O(6)-Ba(2)-Si(1) #4	86.33(9)	O(5)#3-Ba(2)-Si(2) #4	109.4319	O(8)#3-Ba(2)-Si(2) #4	59.29(8)
O(1)#4-Ba(2)-Si(2) #4	25.89(8)	Si(2)-Ba(2)-Si(1) #4	93.1414	Si(2)#3-Ba(2)-Si(2) #4	84.40(3)
O(3)-Si(1)-O(4)	113.7(2)	O(3)-Si(1)-O(1)	110.5(2)	O(4)-Si(1)-O(1)	108.6(2)
O(3)-Si(1)-O(2)	108.5(2)	O(4)-Si(1)-O(2)	110.0(2)	O(1)-Si(1)-O(2)	105.2121
O(3)-Si(1)-Ba(1)	49.08(15)	O(4)-Si(1)-Ba(1)	120.5116	O(1)-Si(1)-Ba(1)	130.86(16)
O(2)-Si(1)-Ba(1)	60.45(16)	O(3)-Si(1)-Ba(1) #6	121.45(16)	O(4)-Si(1)-Ba(1) #6	52.1415
O(1)-Si(1)-Ba(1) #6	57.42(15)	O(2)-Si(1)-Ba(1) #6	130.04(17)	Ba(1)-Si(1)-Ba(1) #6	167.34(5)
O(3)-Si(1)-Ba(2) #4	122.77(16)	O(4)-Si(1)-Ba(2) #4	122.80(160)	O(1)-Si(1)-Ba(2) #4	60.28116
O(2)-Si(1)-Ba(2) #4	44.94(15)	Ba(1)-Si(1)-Ba(2) #4	92.00(41)	Ba(1) #6-Si(1)-Ba(2) #4	100.66(4)
O(3)-Si(1)-Ba(2) #1	35.66(15)	O(4)-Si(1)-Ba(2) #1	80.07(16)	O(1)-Si(1)-Ba(2) #1	113.24(16)
O(2)-Si(1)-Ba(2) #1	134.59(17)	Ba(1)-Si(1)-Ba(2) #1	76.08(3)	Ba(1) #6-Si(1)-Ba(2) #1	91.87(4)
Ba(2) #4-Si(1)-Ba(2) #1	157.01(5)	O(7)-Si(2)-O(1)	110.212	O(7)-Si(2)-O(8)	112.6(2)
O(6)-Si(2)-O(5)	111.2(2)	O(7)-Si(2)-O(5)	107.012	O(6)-Si(2)-O(5)	108.0(2)
O(8)-Si(2)-Ba(2)	126.06(17)	O(15)-Si(2)-Ba(2)	126.21(17)	O(7)-Si(2)-Ba(1) #1	52.20(15)
O(6)-Si(2)-Ba(1) #1	112.85(16)	O(8)-Si(2)-Ba(1) #1	135.95(17)	O(5)-Si(2)-Ba(1) #1	56.24(16)
Ba(2)-Si(2)-Ba(1) #1	81.70(3)	O(7)-Si(2)-Ba(2) #6	124.82(16)	O(6)-Si(2)-Ba(2) #6	124.44(15)
O(8)-Si(2)-Ba(2) #6	56.301161	O(5)-Si(2)-Ba(2) #6	51.42(16)	Ba(2)-Si(2)-Ba(2) #6	177.55(5)
Ba(1) #1-Si(2)-Ba(2) #6	96.02(4)	Si(1)-O(1)-Ba(2) #7	129.7(2)	Si(1)-O(1)-Ba(1) #6	95.88(18)
Ba(2) #7-O(1)-Ba(1) #6	99.91(13)	Si(1)-O(1)-Ba(2) #4	93.83(18)	Ba(2) #7-O(1)-Ba(2) #4	112.61(13)
Ba(1) #6-O(1)-Ba(2) #4	127.31(14)	Si(1)-O(2)-Ba(2) #4	110.4(21)	Si(1)-O(2)-Ba(1)	91.32(18)
Ba(2) #4-O(2)-Ba(1)	125.30(14)	Si(1)-O(3)-Ba(2) #1	123.8(21)	Si(1)-O(3)-Ba(1)	104.78(19)
Ba(2) #1-O(3)-Ba(1)	112.98(14)	Si(1)-O(4)-Ba(2) #6	134.5(2)	Si(1)-O(4)-Ba(1) #6	101.77(19)
Ba(2) #6-O(4)-Ba(1) #6	98.24(12)	Si(2)-O(5)-Ba(1) #1	95.49(19)	Si(2)-O(5)-Ba(2) #6	102.53(19)
Ba(1) #1-O(5)-Ba(2) #6	130.85(15)	Si(2)-O(6)-Ba(2)	95.52(17)	Si(2)-O(6)-Ba(1) #8	129.012
Ba(2)-O(6)-Ba(1) #8	103.80(13)	Si(2)-O(7)-Ba(1)	140.9(2)	Si(2)-O(7)-Ba(2)	97.86(18)
Ba(1)-O(7)-Ba(2)	105.20(13)	Si(2)-O(7)-Ba(1) #1	100.83(19)	Ba(1)-O(7)-Ba(1) #1	101.80113
Ba(2)-O(7)-Ba(1) #1	107.30(14)	Si(2)-O(8)-Ba(1) #4	118.3(2)	Si(2)-O(8)-Ba(2) #6	97.441191
Ba(1) #4-O(8)-Ba(2) #6	136.74(15)				

Symmetry transformations used to generate equivalent atoms: #1: -x+1, -y, -z+2; #2: x, y, z-1; #3: x+1, y, z; #4: -x+1, -y+1, -z+2; #5: x-1, y, z+1; #6: x+1, y, z; #7: x+1, y, z-1; #8: x, y, z+1

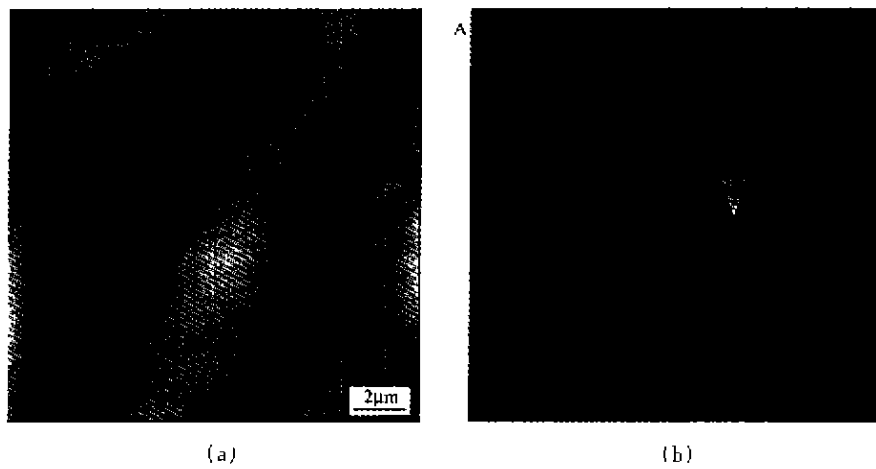


Fig. 3 (a) Surface morphology of the BaH₂SiO₄ single crystal measured using AFM, (b) Domain pattern from the same area shown in (a)

a close packed framework. The short Si-O distance of 1.632 Å produces a tetrahedral environment around Si, and the result is a loosely packed structure of barium atoms and SiO_4 groups. From the feature of the symmetry and composition, it is expected that ferroelectric properties related to the presence of hydrogen bonding in the compound can be obtained. Because its symmetry appears similar to that of the ferroelectric phase of $\text{NaKC}_4\text{H}_4\text{O}_6 \cdot 4\text{H}_2\text{O}$ (seignette salt), which is a single-axis ferroelectric crystal with space group $P2_1$. The spontaneous polarization in seignett salt originates from a -axis. Early work suggested that hydrogen bonding along the a -axis is responsible for the observed ferroelectricity. Neutron diffraction, however, revealed that the preferentially oriented distribution of OH group should be the origin of spontaneous polarization^[10]. In BaH_2SiO_4 , considering the feature of its structure, it is suggested that spontaneous polarization could be observed due to the oriented distribution of OH groups. Further work about neutron diffraction should be done to establish the configuration of hydrogen and then the spontaneous polarization mechanism more firmly.

3 Conclusions

A silicate crystal of BaH_2SiO_4 was grown. It was determined by single-crystal X-ray methods to be triclinic with space group $P\bar{1}$. In this compound, Si atom is surrounded by a tetrahedron of oxygen atoms. The SiO_4 tetrahedron are separated from each other and

bonded by modifier cations of Ba^{2+} . Ferroelectric domain was observed by AFM. The oriented distribution of OH groups along one direction was suggested to be responsible for the observed spontaneous properties.

Acknowledgement: This work was supported by the Center for Smart Materials of the Hong Kong Polytechnic University (under Grant No. A316). The authors would like to thank W. L. Tsui for helpful discussions.

References

- [1] Scott J. F., de Araujo C. A-Paz *Science*, **1989**, *246*, 1400.
- [2] Matsui Y., Okuyama M., Noda M., Harnakawa Y. *Appl. Phys. A*, **1982**, *28*, 161.
- [3] Tokumitsu E., Nakamura R., Ishiwara H. *IEEE Electron Device Lett.*, **1997**, *18*, 160.
- [4] Basit N. A., Kim H. K., Blachere J. *Appl. Phys. Lett.*, **1998**, *73*, 3941.
- [5] Yoshimura M., Yoo S. E., Hagashi M., Ishizawa N. *Jpn. J. Appl. Phys.*, **1989**, *28*, L2007.
- [6] Baesa R. R., Dougherty J. P., Pihone L. J. *Appl. Phys. Lett.*, **1993**, *63*, 1053.
- [7] Chen Q., Zhu J., Li X., Fan C., Zhang Y. *Phys. Lett. A*, **1996**, *220*, 296.
- [8] Brachmann A., Palmer C. E. *Abstract Paper Am. Chem. Soc.*, **2000**, *219*, 145-nucl.
- [9] Haile S. M., Wuensch B. J. *Acta Crystallographica Section B-Structural Science*, **2000**, *56*, 773.
- [10] Frazer B. C., McKeown M., Pepinsky R. *Phys. Rev.*, **1954**, *94*, 1435.